Journal of Hazardous Materials 480 (2024) 136020

Contents lists available at ScienceDirect

Journal of Hazardous Materials

journal homepage: www.elsevier.com/locate/jhazmat

Anaerobic oxidation of methane coupled to reductive immobilization of hexavalent chromium by "*Candidatus* Methanoperedens"

Suicao Wang [a], Xueqin Zhang [a,*], Dihua Tian [b], Jing Zhao [c], Hesamoddin Rabiee [a,d,e], Fangrui Cai [a], Mengying Xie [a], Bernardino Virdis [a], Jianhua Guo [a], Zhiguo Yuan [f], Run Zhang [b], Shihu Hu [a]

[a] *Australian Centre for Water and Environmental Biotechnology (ACWEB), Faculty of Engineering, Architecture and Information Technology, The University of Queensland, Brisbane, Queensland 4072, Australia*
[b] *Australian Institute for Bioengineering and Nanotechnology, The University of Queensland, Brisbane, Queensland 4072, Australia*
[c] *Centre for Mined Land Rehabilitation, Sustainable Minerals Institute, The University of Queensland, Brisbane, Queensland 4072, Australia*
[d] *School of Chemical Engineering, The University of Queensland, Brisbane, Queensland, Australia*
[e] *Centre for Future Materials, University of Southern Queensland, Springfield, Queensland, Australia*
[f] *School of Energy and Environment, City University of Hong Kong, Hong Kong*

HIGHLIGHTS

- '*Ca.* Methanoperedens' enrichment tolerates a Cr(VI) concentration as high as 0.2 mM.
- '*Ca.* Methanoperedens' enrichment couples AOM to Cr(VI) reduction at a theoretical stoichiometry.
- ~94 % Cr(VI) is reduced extracellularly by '*Ca.* Methanoperedens' enrichment.
- '*Ca.* Methanoperedens' couples AOM to Cr(VI) reduction independently.
- Heme proteins of '*Ca.* Methanoperedens' are involved in Cr(VI) reduction.

GRAPHICAL ABSTRACT

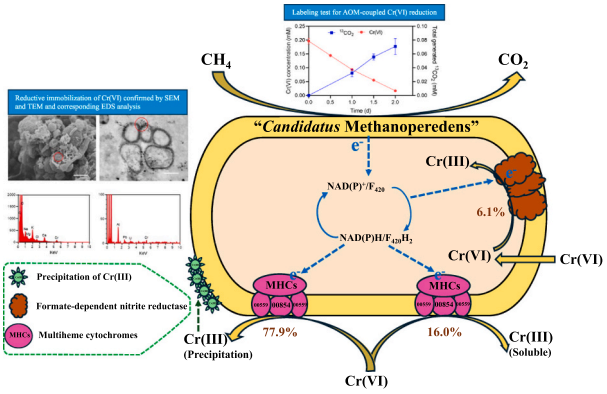

ARTICLE INFO

Keywords:
Anaerobic oxidation of methane
"*Candidatus* Methanoperedens"
Microbial chromate reduction
Multiheme *c*-type cytochrome
Reductase

ABSTRACT

The anaerobic oxidation of methane (AOM) carried out by anaerobic methanotrophic archaea (ANME) plays an important role in mitigating methane emissions from aqueous environments and has applications in bioremediation and wastewater treatment. Previous studies showed that AOM could be coupled to chromate reduction. However, the specific responsible microorganisms and the biochemical mechanisms are unclear. Herein, we showed that a consortium dominated by ANME "*Candidatus* Methanoperedens" was able to couple AOM to the reduction of Cr(VI) to Cr(III) at a stoichiometry close to the theoretical ratio. Quantitative distribution analysis of Cr(III) products suggested Cr(VI) was predominantly reduced via the extracellular respiratory pathways. Further Cr(III)-targeted fluorescent visualization combined with single-cell electron microscopic imaging suggested that

* Corresponding author.
E-mail address: xueqin.zhang@uq.edu.au (X. Zhang).

https://doi.org/10.1016/j.jhazmat.2024.136020
Received 3 July 2024; Received in revised form 3 September 2024; Accepted 29 September 2024
Available online 5 October 2024

Cr(VI) was reduced by "*Ca.* Methanoperedens" independently. Biochemical mechanism investigation via proteomic analysis showed proteins for nitrate reduction under nitrate-reducing conditions were significantly downregulated in Cr(VI)-reducing incubation. Instead, many multiheme cytochrome c (MHCs) were among the most upregulated proteins during the Cr(VI) reduction process, suggesting MHC-governed pathways for extracellular Cr(VI) reduction. The significant upregulation of a formate-dependent nitrite reductase during Cr(VI) reduction indicated its potential contribution to the small proportion of Cr(VI) reduction inside cells.

1. Introduction

Methane (CH_4) is a potent greenhouse gas with a global warming potential approximately 28 times higher than that of carbon dioxide [1]. The global methane cycle is primarily driven by microbial processes, encompassing both methane production and oxidation [2]. Microbial methane oxidation occurring under both aerobic and anaerobic conditions regulates global methane emissions into the atmosphere, with important implications for regulating climate change. In recent decades, the anaerobic oxidation of methane (AOM) has been identified to play an essential role in suppressing methane emissions from anaerobic environments. For example, it was reported that AOM can efficiently consume up to 90 % of the methane produced from ocean sediments [3], whilst it is estimated to decrease potential methane emissions by over 50 % in the world's largest natural methane source of wetlands [4] and lake sediments [5]. AOM is also suggested to be important in the application of bioremediation and wastewater treatment, by utilizing methane as a cheap and renewable energy source [6].

Anaerobic methanotrophic archaea (ANME) have been identified to be the responsible microorganisms for the AOM process. ANME couples AOM to the reduction of various electron acceptors [7,8]. It was initially found that the AOM is coupled with sulfate reduction, involving ANME clusters, primarily ANME-1, ANME-2abc and ANME-3, along with sulfate-reducing bacteria (SRB) [3,9]. Later discoveries have unveiled the coupling of AOM with nitrate reduction by freshwater ANME in the family *Methanoperedenaceae* (formerly ANME-2d) [10,11]. More recently, *Methanoperedenaceae* were confirmed to couple AOM with the reduction of iron oxides, manganese oxides [12], and humic substances [13]. In addition to these proven electron acceptors, thermodynamic calculations and geochemical incubations indicate that AOM can also be linked to the reduction of other electron acceptors, such as selenate [14], chromate [15] and arsenate [16], among others. However, the potential involvement of ANME in the reduction of these electron acceptors and the respective metabolic pathways remains elusive.

Hexavalent chromium (Cr(VI)) is a significant environmental contaminant due to its long persistence in soil and water environments and its high toxicity [17,18]. Cr(VI) exhibits carcinogenic, genotoxic, and mutagenic effects [19,20], owing to its ability to bind with proteins, nucleic acids, and enzymes [21], posing significant health risks to humans and wildlife. Microbes have developed various mechanisms to cope with chromium toxicity, including biosorption, reduction, and bioaccumulation [22]. Cr(VI) reduction results in the formation of Cr (III), which tends to create insoluble hydroxides or oxides under neutral or alkaline pH conditions [23,24]. This reduces its potential for migration and environmental toxicity [25].

It was recently proposed that Cr(VI) reduction to Cr(III) could be coupled with AOM according to the following thermodynamically feasible reaction [7]:

$$3CH_4 + 8CrO_4^{2-} + 16\ H^+ \rightarrow 4Cr_2O_3 + 3CO_2 + 14\ H_2O\ (\Delta G_0' = -708\ kJ\ mol^{-1}\ CH_4) \quad (1)$$

Therefore, AOM might be coupled with the immobilization of chromium under methane-rich conditions, and this may be an important biogeochemical process that has been overlooked in natural environments.

Microbial Cr(VI) reduction coupled with AOM has been investigated in three studies [15,26,27], all of which have addressed the feasibility of this process, but did not answer the underlying mechanistic questions: what is the nature of the microbes involved and how is the process achieved? Two works observed the Cr(VI)-dependent AOM by *Methanoperedenaceae*-enriched consortia, in which *Methanoperedenaceae* is the only microorganism encoding the methane-metabolizing pathways [15,27]. Thus, it was speculated in both papers that *Methanoperedenaceae* may have carried out observed Cr(VI)-dependent AOM independently, while the biochemical mechanisms were not studied. Meanwhile, as both works observed the appearance and enrichment of new bacteria genera in the microbial community after Cr(VI) reduction, it was also speculated that *Methanoperedenaceae* symbiotically worked with newly appeared bacteria (suggested as putative Cr(VI) reducers) via a cross-feeding pathway through diffusion of AOM-derived intermediates produced by *Methanoperedenaceae*. In another work [26], Cr (VI)-dependent AOM was achieved in a methane-based membrane biofilm reactor (MBfR), with methanogens (*Methanobacterium* and *Methanosarcina*) and ANME (*Methanoperedenaceae*) enriched as putative anaerobic methane oxidizers, and *Meiothermus* as putative bacterial Cr (VI) reducer. It was speculated that methanogens/ANME anaerobically oxidized methane and released electrons for Cr(VI) reduction by *Meiothermus*. In summary, responsible microorganisms and the biochemical mechanisms for AOM coupled with Cr(VI) reduction were not unambiguously elucidated in previous studies.

This study aims to distinguish the independent and syntrophic pathways for Cr(VI)-dependent AOM and resolve whether this process could be performed by ANME independently. Moreover, the biochemical mechanisms are investigated for the Cr(VI) by ANME. To achieve these aims, we first investigated stoichiometric coupling between AOM and Cr(VI) reduction by a "*Ca.* Methanoperedens" enrichment culture in batch incubations. Cr(III)-targeted fluorescent visualization with confocal microscopy was used to target the Cr(VI) reducers in the community and single-cell electron microscopic imaging including transmission electron microscope with energy dispersive X-ray (TEM-EDS), and scanning electron microscopy with energy-dispersive X-ray spectroscopy (SEM-EDS) were used to visualize the deposition of Cr(III) products on the surface of Cr(VI) reducers. Additionally, we conducted the proteomic analysis to compare the protein expression under the Cr (VI)-reducing condition and the nitrate nitrate-reducing condition to probe the chemical mechanisms for Cr(VI)-dependent AOM by "*Ca.* Methanoperedens".

2. Materials and methods

2.1. Inoculum and culture medium

The inoculum used for microcosm incubation in this study was collected from a 2 L parent bioreactor with a working volume of 1.6 L. The consortium in the bioreactor was enriched with "*Ca.* Methanoperedens" to perform nitrate-dependent AOM [10]. The parent bioreactor was operated at a constant temperature of 24 ± 2 °C, and the pH was controlled at around 7.0 by adjusting with 1 mol/L NaOH or 1 mol/L HCl. A mineral salts medium (composition consisted of the following components (unit: g/L)): KH_2PO_4 (0.075), $MgSO_4 \bullet 7H_2O$ (0.2), $CaCl_2 \bullet 2H_2O$ (0.3), and trace elements [28] was used for the cultivation of biomass and maintenance of a relatively stable microbial community of the parent bioreactor. The bioreactor was intermittently fed with nitrate, ammonium, and methane according to details reported

previously [29], and it showed an average NO_3^--N and NH_4^+-N removal rates of approximately 2.0 mmol/L d^{-1}.

2.2. Microcosm incubations

2.2.1. Incubations to test the effect of initial Cr(VI) concentration

The tolerance of "*Ca.* Methanoperedens" enriched culture to different Cr(VI) concentrations (0.1, 0.2, 0.5, 1.0, and 2.0 mmol/L) was tested so that an appropriate Cr(VI) concentration could be used for the following Cr(VI) reduction experiments. The biomass collected from the parent bioreactor was first incubated in a 210-mL anoxic vessel to consume the residual nitrate. 15 mL of nitrate-depleted "*Ca.* Methanoperedens" enrichment culture was then inoculated into 23-mL serum bottles, combined with an anoxic and filtered stock solution of potassium chromate (100 mmol/L chromium) to the desired concentrations. After capping serum bottles with butyl rubber stoppers and aluminum caps, bottles were injected with a methane-based mixed gas (90 % CH_4, 5 % CO_2, 5 % N_2, Coregas, Australia) as the sole electron donor. All the above procedures were conducted in an anaerobic glove chamber (22 ± 2 ℃, Coy Laboratory Products Inc., USA). All experiments were run in triplicate and incubated on a shaker (RATEK, Australia) at a constant temperature of 24 ± 2 °C, with shaking at 100 rpm. During the experiment, biomass samples were taken every 12 h for the first 48 h. A 0.5 mL of biomass suspension was collected from each serum bottle, which was centrifuged at 10,000 rpm for 2 min. The supernatant was analyzed for Cr(VI), and the solid pellet was stored for future analysis.

2.2.2. Incubations for isotope tracer assay

To confirm the coupled AOM with Cr(VI) reduction and calculate the corresponding stoichiometry, an isotope tracer assay was conducted with microcosm incubation by feeding ^{13}C-CH_4 and Cr(VI). Incubations were conducted in triplicate in 23-mL serum bottles with 15 mL of nitrate-free inoculum from the parent bioreactor as inoculum in each bottle. Cr(VI) stock solution was injected into each bottle, resulting in a final concentration of 0.2 mmol/L Cr(VI). After sealing these bottles with butyl rubber stoppers and aluminum caps, 8 mL of headspace gas was replaced with the methane-based mixed gas as noted above, and an additional 5 mL of $^{13}CH_4$ (>99 %, Sigma Aldrich) was injected into the bottle. Meanwhile, a control group was established using the same inoculum and experimental setup but with nitrate (at an initial concentration of ~6.0 mM) as the electron acceptor. 8 mL of headspace gas was replaced with the methane-based mixed gas as noted above and an additional 5 mL $^{13}CH_4$ gas was injected. Finally, all serum bottles were incubated at 100 rpm in the incubator shaker, and the temperature was maintained at 24 ± 2 °C. Geochemical measurements were performed on subsamples of the anoxic microcosms over a 48-hour period. 0.3 mL of supernatant was subsampled from each microcosm after 2 h, 12 h, 24 h, 36 h, and 48 h after initial setup. Sampled biomass was centrifuged at 10,000 rpm for 2 min. The supernatant was used for Cr(VI) measurement. Another 0.5 mL of biomass was sampled at 2 h, 24 h, 36 h, and 48 h, then injected into 3-mL Exetainer vials (Labco, UK) that had been previously flushed with helium gas for 5 min, and these samples were stored at −20℃ for $^{13}CO_2$ measurement.

2.3. Chromium distribution, fates, and mass balance analysis for microbial Cr(VI) reduction

Cr(VI) reduction can be achieved by microorganisms inside cells or outside cells. Here, we performed a quantitative mass balance for the Cr (VI) reduction to resolve the spatial distribution of chromium products produced from Cr(VI) reduction, including intracellular Cr, extracellular Cr(III) in soluble form in the solution (Soluble Cr(III) in solution) and extracellular Cr(III) bound on the cell surface (Surface Cr(III)). Microcosm incubation at 0.2 mmol/L initial Cr(VI) concentration as noted above was used to analyze the chromium distribution throughout the Cr (VI)-reducing course. The supernatant of each sample was subjected to quantifying the concentrations of dissolved Cr(VI) and total aqueous chromium. The difference between total aqueous chromium and Cr(VI) in solution was categorized as Soluble Cr(III) in solution. To quantity the Cr(III) products precipitating on the cell surface (Surface Cr(III)), the biomass pellet for each sample was subjected to chromium extraction using 6 mol/L HCl for 2 h [30], and total chromium was subsequently determined to represent the partial chromium that was reduced by "*Ca.* Methanoperedens" enriched culture with extracellular pathways. To quantify the intracellular Cr(VI) reduction products (Intracellular Cr (III)), the solid biomass pellet previously extracted with 6 mol/L HCl, was subjected to microwave digestion in 14.4 mol/L HNO_3 at 150 ℃ for 20 min. The resulting digest solution was then used to determine the total chromium content as a representative of chromium that was reduced by "*Ca.* Methanoperedens" enriched culture with intracellular pathways.

To further understand the fate of microbial Cr(VI) reduction by the "*Ca.* Methanoperedens" consortium, the speciation of extracellular Cr was analysed by X-ray Photoelectron Sppectroscopy (XPS) after Cr(VI) reduction was performed. A Kratos Axis Ultra X-ray photoelectron spectrometer (Manchester, UK) was employed to collect XPS spectra with a monochromatized Al Kα x-ray at 150 W.

2.4. Fluorescent visualization to distinguish the independent Cr(VI) reduction by "Ca. Methanoperedens"

To discriminate whether "*Ca.* Methanoperedens" in the consortium is capable of Cr(VI) reduction independently, or if it relies on syntrophic interdependent Cr(VI) reducers for Cr(VI) reduction [15], a fluorescent method was set up by using Cr(III)-selective chemosensory fluorescence and the autofluorescence of "*Ca.* Methanoperedens". The principle of this method can be summarized as follows. Chromium products generated from microbial chromate reduction can be absorbed and accumulated on cell surfaces of Cr(VI) reducers [30,31]. Therefore, Cr (VI)-reducing microorganisms can be lighted with Cr(III)-specific probes and visualized via Cr(III) chemosensory fluorescence [32]. Meanwhile, "*Ca.* Methanoperedens" cells can be visualized and distinguished in the consortium by the autofluorescence of cofactor F_{420} [33]. Probe synthesis was performed based on an existing method [32]. Details information on fluorescent staining and visualization of the probe for Cr(III) and other metal ions can be found in the Supplementary Materials.

2.5. Electronic microscopic visualization of Cr(III) deposition on cell outermost surface

As "*Ca.* Methanoperedens" cells can be distinguished from other cells in the consortium with electronic microscopy (identified by their distinctive morphology and size) [34], electronic microscopic methods were performed to further confirm whether "*Ca.* Methanoperedens" can reduce Cr(VI) independently by visualizing the potential precipitation of Cr(III) products on its cell surface. Biomass from Cr(VI) incubation was collected to have single-cell visualization of Cr deposition on "*Ca.* Methanoperedens" cells using scanning electron microscopy (SEM) and sectioning transmission electron microscopy (TEM). Details of SEM and TEM samples preparation and microscopic visualization are shown in the Supplementary Materials.

2.6. Proteomic analysis

To further investigate the metabolic mechanisms of Cr(VI)-dependent AOM, especially the biochemical machinery for Cr(VI) reduction by "*Ca.* Methanoperedens", a new incubation was established to perform the proteomic analysis under the Cr(VI)-reducing condition in comparison to that under the nitrate-reducing condition. Incubations with Cr(VI) and nitrate as terminal electron acceptors were set up in triplicate the same as the details described in Section 2.2.2. 8 mL of

headspace gas was replaced in each serum bottle with the methane-based mixed gas as noted above to provide the electron donor. The supernatant was subsampled from incubation at different intervals to monitor Cr(VI) and nitrate reduction. After 48 h, 8 mL microcosms were collected from each serum bottle and immediately centrifuged (7500 rpm for 10 min at 4 ℃) to pellet the cells. The pellets were then washed with PBS (x1) twice and immediately stored at −80℃ before being analyzed. Sample preparation and proteomic analysis were conducted by Queensland Metabolomics and Proteomics (Q MAP) following established protocols [35].

2.7. Quantification of MHC contents

To probe the essential role of MHCs in Cr(VI) reduction by "*Ca.* Methanoperedens", MHC content of the biomass was specifically quantified under the Cr(VI)-reducing condition in comparison to that under the nitrate-reducing condition. 2 mL biomass sample was collected from the aforementioned incubation for the proteomic experiment at the 48th hour and centrifuged at 7500 rpm for 2 min to harvest the biomass pellet. After washing with 1 x PBS twice, the biomass pellet was lysed in a Lysing Matrix E tube (MP Biomedicals, US) on a bead-beating grinder (FastPrep® Instrument) for 40 s at a setting of 6.0. After centrifugation at 7500 rpm for 2 min, the supernatant was used for quantification of heme contents using a spectrophotometric method [36]. Meanwhile, the supernatant was also used for the quantification of protein contents using a corrected Lowry method [37].

2.8. 16S rRNA amplicon sequencing and analyses

In the isotope tracer experiment, 0.5 mL biomass samples were collected from both control and target groups at the beginning and end of the incubation course (48 h) to investigate potential changes in the microbial community structure via 16S rRNA gene amplicon. DNA was extracted and sequenced by the Australian Center for Ecogenomics (ACE) using 16S amplicon sequencing at the University of Queensland. The universal primer set of 926 F (5′-AAACTYAAAKGAATTGACGG-3′) [38] and 1392 R (5′-ACGGGCGGTGWGTRC-3′) was used to amplify V6-V8 regions of the 16S rRNA genes. Amplicons were sequenced by Illumina Miseq Platform and analysed using the ACE pipeline (https://wiki.ecogenomic.org/doku.php?id=amplicon_pipeline_readme). This pipeline comprises a quality control module, amplicon clustering by QIME2, and taxonomy assignment on representative OUT sequences through BLAST [39,40]. The above sequencing results have been deposited in the NCBI database with the accession No. PRJNA1155252.

2.9. Chemical analyses

The concentration of Cr(VI) in the supernatant was measured using an ultraviolet-visible spectrophotometer (UV-Vis) at 540 nm using 1, 5-diphenylcarbazide as the reagent, following the methodology described in a previous study [41]. Total chromium was measured using an Inductively Coupled Plasma-Optical Emission Spectroscopy (ICP-OES, Thermo Fisher iCap Pro), at the absorption wavelength of 267.716 nm. The concentrations of nitrate, nitrite, and ammonia for samples were determined using a Flow Injection Analyzer (FIA, QuickChem 8000, Lachat Instrument, Milwaukee, WI). Liquid samples were collected from the batch tests using sterile syringes and needles, then they were immediately centrifuged at 10,000 g for 2 min to separate biomass pellets and supernatant. The partial pressures of methane were quantified using a Shimazu gas chromatograph (GC, Porapak Q column) [39]. For the quantification of $^{13}CO_2$ produced from $^{13}CH_4$, Exetainer vials stored were thawed and subsequently acidified with 0.2 mL of anaerobic HCl solution (5 mM) and shaken for at least 2 h before conducting gas chromatography-mass spectroscopy (GC/MS) analysis. The ^{13}C isotopic ratio of CO_2 in the headspace of the Exetainer vials was measured using GC/MS (GC7890A coupled to MSD 5975 C; Agilent) according to details in a previous work (Zhang et al., 2020). The total $^{13}CO_2$ production for each sample was calculated as described by previous research [42].

3. Results and discussion

3.1. Effect of initial Cr(VI) concentrations on Cr(VI) reduction

High concentrations of Cr(VI) can be toxic to microorganisms, and the microbial Cr(VI) reduction can be inhibited at elevated concentrations, as observed for Cr(VI)-reducing bacteria *Comanonas testosteroni* [43], *Bacillus* spp. [44] and *Geobacter* spp. [30]. Previous studies observed the Cr(VI) reduction by "*Ca*. Methanoperedens" enrichment cultures at low Cr(VI) concentrations of 10 μmol/L [15] and 20 μmol/L [27], while the potential inhibitory effect of elevated concentrations of Cr(VI) on Cr(VI) reduction by "*Ca*. Methanoperedens" enrichment cultures was unknown. Herein, the effect of the initial concentration of Cr (VI) on its reduction kinetics by "*Ca.* Methanoperedens" enrichment culture was investigated within a concentration range of 0.1 to 2.0 mM of Cr(VI), including 0.1, 0.2, 0.5, 1.0, and 2.0 mM (Fig. 1). The Cr(VI) reduction rate was observed to slightly increase from 0.076 ± 0.005 to 0.083 ± 0.002 mmol/L/d when the initially available Cr(VI) was increased from 0.1 to 0.2 mM (Fig. 1). This phenomenon can be explained by the Michaelis-Menten dynamic model [45], which indicates that at low concentrations, the rate of Cr(VI) consumption increases with increasing initial Cr(VI) concentration. The similar phenomenon was previously observed for microbial Cr(VI) reduction mediated by other microorganisms such as *P. saccharolyticum* strain LY10 [46] and CRB-7[47]. The Cr(VI) reduction rate started to drop when the initial concentration of Cr(VI) was further increased, representing 0.078 ± 0.005 mmol/L/d, 0.059 ± 0.009 mmol/L/d, and 0.032 ± 0.009 mmol/L/d for initial Cr(VI) concentrations of 0.5, 1.0, and 2.0 mM, respectively. These results show that "*Ca*. Methanoperedens" enrichment culture can tolerate a Cr(VI) concentration as high as 0.2 mmol/L, and Cr(VI) reduction activities can be significantly inhibited at Cr(VI) concentrations higher than 0.5 mmol/L. A similar tolerance level of Cr(VI) has also been found in representative Cr(VI)-reducing bacteria, such as *Geobacter sulfurreducens* PCA [30], *Shewanella putrefaciens* 200 [48], *CRB6* [49]. Based on these results, we then applied an initial concentration of 0.2 mmol/L in our subsequent experiments in an attempt to minimize the inhibitory impact of Cr(VI) on the "*Ca.* Methanoperedens" enrichment culture.

3.2. AOM coupled with Cr(VI) reduction confirmed by isotope tracer experiment

To determine whether the observed Cr(VI) reduction by "*Ca.*

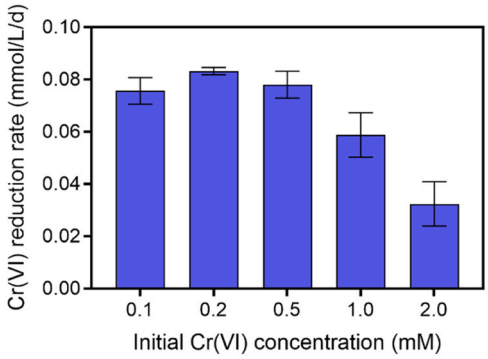

Fig. 1. Effects of different initial Cr(VI) concentrations (including 0.1, 0.2, 0.5, 1.0, and 2.0 mM) on the Cr(VI) reduction rates by "*Ca.* Methanoperedens" enrichment culture. The Cr(VI) reduction rates were obtained by linear regression of the Cr(VI) consumption data collected during the first 48 h of the experiment (Fig. S1).

Methanoperedens" enrichment culture was driven by AOM and to identify the corresponding stoichiometry, we performed an isotope tracer experiment during which $^{13}CH_4$ was fed to the Cr(VI)-reducing incubations. As shown in Fig. 2, along with the gradual Cr(VI) consumption from 0.196 ± 0.011 to 0.017 ± 0.003 mM observed within the 48 h of incubation, the total generated $^{13}CO_2$ produced from $^{13}CH_4$ was observed to gradually increase from 0 to 0.071 ± 0.017 mM (see detailed calculation in the Supplementary Material). The Cr(VI) reduction rate during this period was 0.090 ± 0.004 mmol/L/d, and the $^{13}CO_2$ was accumulated at a rate of 0.036 ± 0.005 mmol/L/d (Fig. S2a). The Cr(VI) reduction and $^{13}CO_2$ accumulation (from $^{13}CH_4$ consumption) was at a ratio of 0.402, which was close to the theoretical stochiometric ratio of 3:8 (Eq. 1), suggesting the coupling of AOM with Cr (VI) reduction by the "*Ca.* Methanoperedens" enrichment culture. The ratio of Cr(VI) reduction to $^{13}CH_4$ consumption (0.402) is slightly higher than the theoretical value, which could be explained by the potential synthesis of polyhydroxyalkanoate (PHA) or acetate to provide additional electron sink during AOM by '*Ca.* Methanoperedens' [29]. In this process, CH_4 is the only energy source (electron donor), and both CH_4 and CO_2 could be the carbon sources, which warrant further studies with physiological evidence to prove.

3.3. Fate and quantitative distribution of Cr(VI) reduction mediated by "Ca. Methanoperedens" enrichment culture

To investigate the products of microbial Cr(VI) reduction, XPS analysis was employed to identify the presence and valence state of chromium at the end of the incubations. Contrasting with the inoculum biomass, the high-resolution XPS spectra of biomass after Cr(VI) reduction showed two distinct Cr-featured peaks at 576–577 eV (Cr(III) 2p3/2) and 587 eV (Cr(III) 2p1/2) (Fig. 3a). This result is similar to the Cr(VI)-reducing products previously reported for *Geobacter sulfurreducens* [30] and *Aeromonas hydrophila* [31], demonstrating that Cr(VI) reduction by "*Ca.* Methanoperedens" enrichment culture results in the products mainly of Cr(III) compounds.

Cr(VI) reduction can be achieved by microorganisms inside cells or outside cells via intracellular or extracellular respiratory pathways [30]. The spatial analysis of the Cr(VI) reduction products to discriminate their intracellular and extracellular distributions could inform on the Cr (VI) reduction pathways of "*Ca.* Methanoperedens". To this end, we performed a quantitative mass balance for the Cr(VI) reduction to indicate the distribution of intracellular, soluble (i.e., in solution), and surface-bound Cr(III). Results are presented in Fig. 3b, with calculations reported in Supplementary Materials and additional results shown in Table S1. A small proportion (3.7 ± 1.7 % and 6.8 ± 2.9 % at 24 h and 48 h, respectively) of Cr(III) was distributed intracellularly when Cr(VI) was reduced by "*Ca.* Methanoperedens" enrichment culture, representing only 6.4 ± 2.0 % and 6.1 ± 2.7 % of total reduced chromium at 24 h and 48 h, respectively. In comparison, the majority (nearly 94 %) of the reduced chromium was distributed extracellularly, as insoluble Cr(III) on the cell surface or soluble Cr(III) in solution. 35.4 ± 1.0 % and 87.0 ± 0.8 % of the reduced chromium was observed to be distributed on the cell surface of microbial samples collected at 24 h and 48 h, respectively, which separately represented 60.5 ± 8.4 % and 77.9 ± 1.9 % of the total reduced chromium.

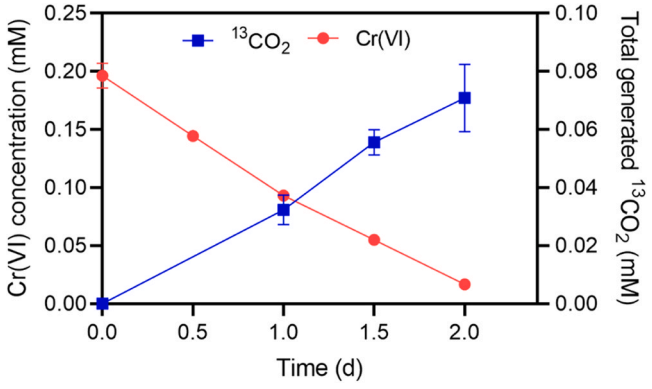

Fig. 2. Dynamic changes of the concentrations of Cr(VI), and the total generated $^{13}CO_2$ from $^{13}CH_4$-labeled Cr(VI)-reducing incubation (Calculations of $^{13}CO_2$ generation were outlined in the Supplementary Material). Results from three independent biological replicates are represented as mean ± SD.

This dominance of extracellular distribution of Cr(III) species was also observed previously in *G. sulfurreducens PCA* [41] and *Aeromonas hydrophila* [31], both of which were attributed to their extracellular respiratory pathways. As such, the XPS and quantitative distribution analysis reported here, in particular, the observation that the majority of products from the Cr(VI) reduction are insoluble Cr(III) on the cell surface, suggest that Cr(VI) could be reduced mainly due to the extracellular respiratory pathways of "*Ca.* Methanoperedens" enrichment culture.

3.4. Fluorescence visualization of independent Cr(VI) reduction by "Ca. Methanoperedens"

Two recent works reported on the feasibility of Cr(VI) reduction by "*Ca.* Methanoperedens" enrichment cultures, and both works observed the appearance and enrichment of new bacterial genera within the microbial community following Cr(VI) reduction, which were indicated to be putative Cr(VI) reducers [15,27]. On this basis, both papers speculated two possible mechanisms for Cr(VI) reduction: 1) "*Ca.* Methanoperedens" independently couple AOM to Cr(VI) reduction, through currently unknown biochemical pathways; 2) "*Ca.* Methanoperedens" forms a syntrophic association with unidentified bacterial Cr(VI) reducers whereby the latter couples Cr reduction with the oxidation of AOM-derived intermediates (e.g., acetate). Contrasting with previous papers, in this study, the microbial community in microcosm incubations in the presence of Cr displayed no significant shift in community profile when compared to the nitrate-enriched inoculum (Fig. S3). This seems to reconcile the scenario where Cr(VI) is reduced independently by "*Ca.* Methanoperedens" (*i.e.*, through mechanism #1 discussed above). To further prove this hypothesis, we conducted a Cr (III) fluorescence staining experiment to identify the microorganisms directly responsible for the observed Cr(VI) reduction. Cr(III) produced by Cr(VI) reducer can be coordinated with the functional groups on the cell surface and create a layer of accumulated Cr(III) on the surface of Cr (VI) reducer [30,31]. Therefore, a Cr(III)-selective fluorescent chemosensor can be lighted by Cr(III) for the fluorescent visualization of Cr(VI) reducers. As a significant amount of Cr(III) was distributed on the cell surface after Cr(VI) reduction (Fig. 3b), Cr(III)-selective fluorescent chemosensor would enable the identification of Cr(VI) reducers in the "*Ca.* Methanoperedens" enrichment culture.

To achieve this experimental purpose, a Cr(III)-selective turn-on fluorescent probe (RB-CR) was firstly synthesized according to the method described by Jiang et al., which was previously used to stain and image Cr(III) in living cells [32]. ^{1}H NMR and ^{13}C NMR analysis confirmed the successful synthesis of RB-CR (Fig. S4a, b). A significant turn-on fluorescence change of RB-CR can be observed under the trigger of Cr(III) instead of Cr(VI) (Fig. S4c), and this trigger was selective to Cr (III) but not other metal ions that could exist in the medium of Cr (VI)-reducing incubations (Fig. S4d). These results combined confirm the feasibility and selectivity of RB-CR synthesized in this study for Cr (III)-selective fluorescent chemosensor.

When applied to biological samples taken at the end of the Cr(VI)-reducing incubations, the "*Ca.* Methanoperedens" cells (visualized with autofluoresce, Fig. 4a) exhibited a noticeable Cr(III)-selective fluorescent response to staining with RB-CR (Fig. 4b). Remarkably, the cells that positively stained with RB-CR mostly overlapped with autofluoresced "*Ca.* Methanoperedens" cells (Fig. 4c, Fig. S5). Moreover, it

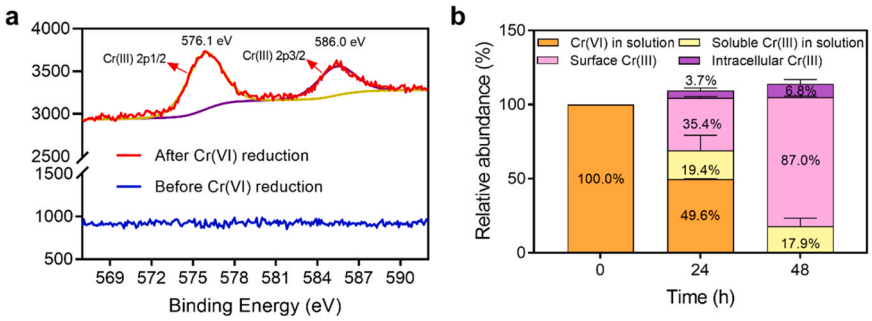

Fig. 3. Characterization of the reduced products of Cr(VI) reduction by "*Ca.* Methanoperedens" enrichment culture. **a** XPS analysis of "*Ca.* Methanoperedens" enrichment biomass before and after Cr(VI) reduction. **b** The time-dependent distribution of Cr in the batch incubation for Cr(VI) reduction by "*Ca.* Methanoperedens" enrichment culture. Results from three independent biological replicates are represented as mean ± SD.

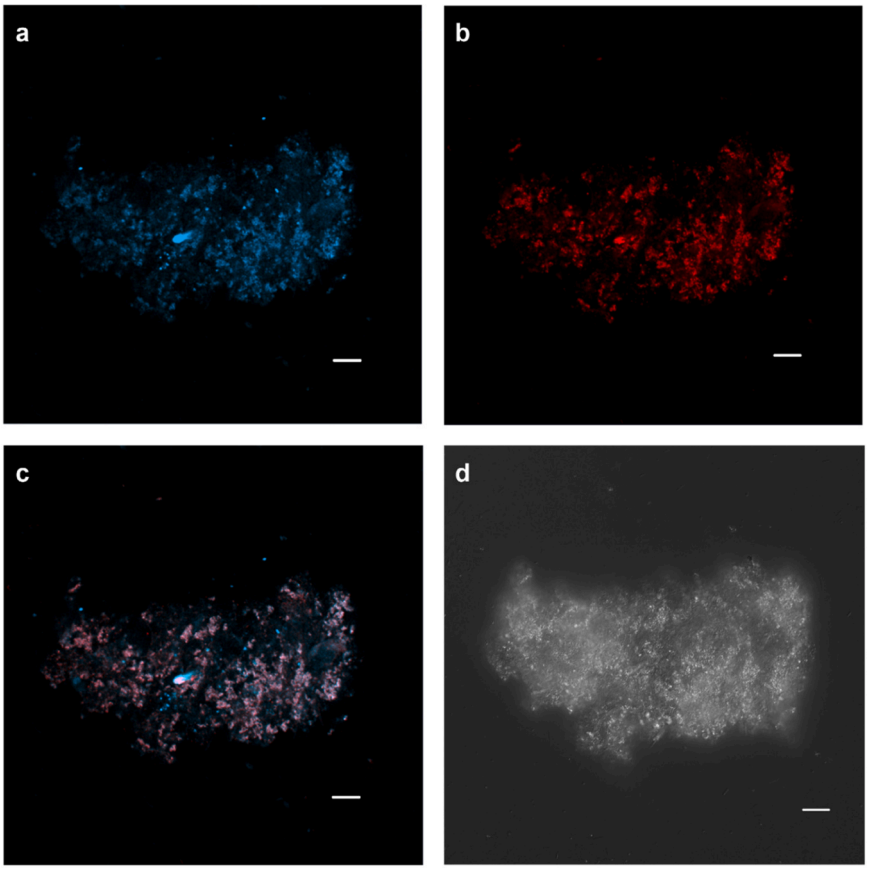

Fig. 4. Fluorescent characterization of "*Ca.* Methanoperedens" performed at the end of the incubations in the presence of Cr(VI). **a** The autofluorescence image of methanogenic cofactor F_{420}, representing "*Ca.* Methanoperedens" cells, **b** The fluorescence image of cells stained with RB-CR, representing Cr(VI)-reducing cells in the consortium, **c** Overlay of the fluorescent images **a** and **b**, **d** Phase-contrast micrograph at the corresponding fields of view**.** Scale bars indicate 10 μm.

can be found from the phase-contrast micrograph that other cells co-exist with "*Ca.* Methanoperedens" cells in the consortium (Fig. 4d), while these accompanying cells were not stained with RB-CR (Fig. 4b). Overall, the fluorescent staining results supported the hypothesis that "*Ca.* Methanoperedens" was independently responsible for Cr(VI) reduction and did not need a symbiotic association with a separate Cr (VI) reducer.

3.5. Microscopic characterization of Cr(VI) reduction by "Ca. Methanoperedens"

Due to the distinctive morphology of "*Ca.* Methanoperedens" (irregular cocci shape at larger size to other populations; typically found as sarcina-like clusters), "*Ca.* Methanoperedens" cells can be distinguished from other cells in the enrichment culture through microscopic visualization [34]. To further confirm the independent Cr(VI) reduction by "*Ca.* Methanoperedens", microscopic characterization with both SEM and TEM was performed to visualize the localizations of reduced Cr(III) precipitates potentially on "*Ca.* Methanoperedens" cell surface. In comparison to the SEM morphology showing the smooth surface of "*Ca.* Methanoperedens"-like cells from the inoculum (Fig. 5a), the cells with a rough surface coated with precipitates were observed after Cr(VI) incubation (Fig. 5b). Furthermore, analyses of these cell envelope-associated precipitates with SEM-coupled EDX confirmed the presence of chromium exclusively on the rough "*Ca.* Methanoperedens"-like cell surface (Fig. 5f), contrasting with no detectable

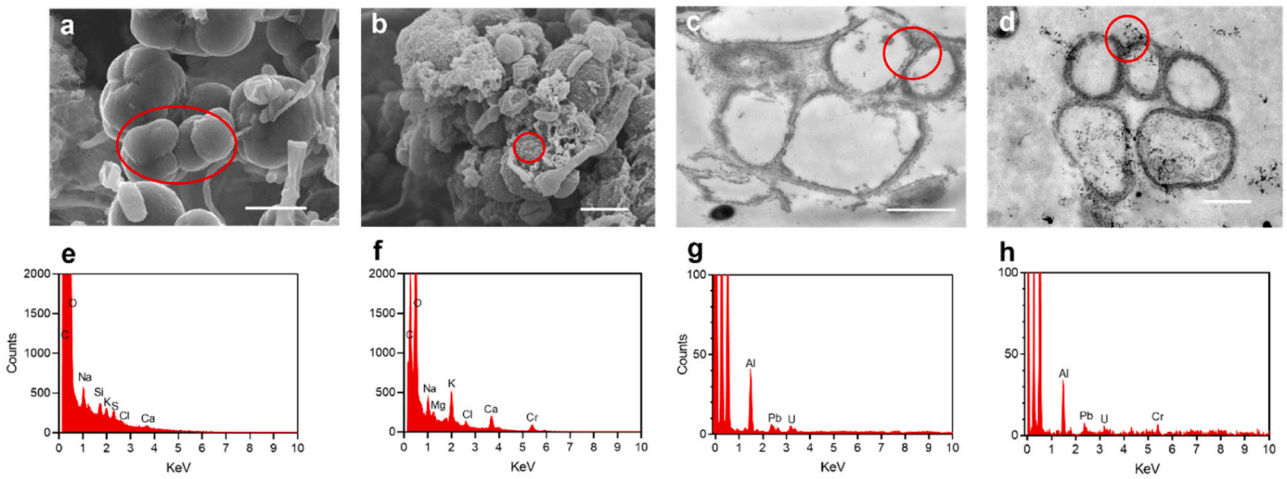

Fig. 5. Microscopic characterization of Cr(VI) reduction by "*Ca.* Methanoperedens". **a**, **b** SEM images show the characteristics of the "*Ca.* Methanoperedens" cell (identified by their distinctive morphology and size) surfaces in the inoculum and in the Cr(VI)-reducing incubation, respectively. **e, f** Elemental information within the red circles via EDS analysis corresponding to **a** and **b**, respetively. **c, d** TEM images display the extracellular features of the "*Ca.* Methanoperedens" cells in the inoculum and under the Cr(VI)-reducing incubation, respectively. **g, h** Elemental analysis of the red circle areas using EDS analysis corresponding to images **c** and **d**. Scale bars indicate 1 μm.

chromium on the smooth cell surface from the inoculum (Fig. 5e). Compared to "*Ca.* Methanoperedens" cells grown without Cr(VI) reduction (Fig. 5c), the cell surface with Cr(VI) reduction contains many dark electron-dense areas (Fig. 5d). STEM analysis results support that Cr appears in these dark areas (Fig. 5h), contrasting with no Cr signals in the similar areas (red circle) in Fig. 5g. Overall, cellular locations of reduced Cr(III) precipitates combined with EDS analysis further corroborate the involvement of "*Ca.* Methanoperedens" in Cr(VI) reduction, mainly through extracellular respiratory pathways.

3.6. Biochemical mechanisms for microbial Cr(VI) reduction by "Ca. Methanoperedens"

Microbial Cr(VI) reduction has been previously reported for diverse microorganisms using intracellular or extracellular strategies according to the site of occurrence [50]. For intracellular processes, it was proposed that Cr(VI) is reduced in the cytosol using cytoplasmic soluble reductase enzymes such as NADH, NADPH, cytochrome c3 [50]. In addition, several oxidoreductases with other different metabolic functions, including nitroreductase, quinone reductases, and NAD(P)H-dependent reductases [51], can also catalyse Cr(VI) reduction. In contrast, the extracellular reduction of Cr(VI) followed by Cr(III) binding with functional groups on the cell surface is a strategy used by some microorganisms to cope with Cr(VI) toxicity [52]. Extracellular reduction is normally associated with membrane-bound reductases such as flavin reductases, hydrogenases and cytochromes that are part of the electron transport system and use chromate as the terminal electron acceptor [51]. Some organisms capable of extracellular electron transfer (EET) have been reported to be able to reduce Cr(VI) using this mechanism [31,53–55]. The specific biochemical pathway has been elucidated for *Shewanella oneidensis* MR-1, in which extracellular MHCs including MtrC and OmcA were reported to be the terminal reductases used for extracellular Cr(VI) reduction and OmcA is identified as the predominant Cr(VI) reductase [56]. The MtrC homologue is also suggested as the predominant extracellular reductase for extracellular Cr(VI) reduction by *Aeromonas hydrophila* [31]. "*Ca.* Methanoperedens" was recently identified to be another EET-capable candidate, which has been shown with extracellular respiratory flexibility with different extracellular electron acceptors [39,57–61]. Moreover, a recent study confirmed that MHCs enable extracellular respiration of "*Ca.* Methanoperedens", and remarkably, "*Ca.* Methanoperedens" can regulate the expression of MHCs to adapt its versatile respiratory pathways to the extracellular reduction of different terminal electron acceptors [34,62]. Therefore, we proposed that "*Ca.* Methanoperedens" may also use its special MHC-mediated extracellular respiration pathways for the observed extracellular Cr(VI) reduction (Figs. 3b, 4c, 5b, 5c).

To gain a system-wide understanding of the biochemical mechanisms for microbial Cr(VI) reduction by "*Ca.* Methanoperedens", proteomic analysis was conducted to compare differences in protein expression of "*Ca.* Methanoperedens" in Cr(VI)-reducing versus nitrate-reducing incubations. Proteome composition reflected the availability of the principal energy source and terminal electron transfer pathway under each condition (Fig. 6, Supplementary datasheet). Some proteins involved in central carbon- and energy metabolisms, cellular status maintenance and electron transfer pathway for Cr(VI) reduction in "*Ca.* Methanoperedens" significantly differed from the cells at nitrate-reducing incubation. "*Ca.* Methanoperedens" is prevalently proposed to use a reverse methanogenesis pathway for AOM [63,64]. Associated proteins governing this pathway, especially the key proteins of methyl-coenzyme M reductases (Mcr), were highly expressed in the Cr(VI)-reducing incubation (Fig. 6a), suggesting "*Ca.* Methanoperedens" also uses the reverse methanogenesis pathway for Cr(VI)-driven AOM activity (Fig. 2). Mcr proteins were found to be downregulated significantly, with McrA and McrB only 0.7- and 0.6-fold (Fig. 6a), respectively, under the Cr(VI)-reducing condition in comparison to the nitrate-reducing condition. This was in line with the observation of decreased AOM activity (0.036 ± 0.0048 mmol/L/d; Fig. S2a) in Cr(VI) incubation in comparison with the activity of methane oxidation (0.209 ± 0.0075 mmol/L/d; calculation in Supplementary Material) in nitrate incubation during the period of isotopic tracing experiment. Most of the other proteins involved in central AOM pathways, including 5,10-methylenetetrahydromethanopterin reductase (Mer), Methyl-coenzyme M reductase alpha subunit (McrA), and Methyl-coenzyme M reductase beta subunit (McrB), down-regulated to 0.6-, 0.7-, and 0.7-fold, respectively.

Interestingly, contrasting with the significant down-regulation of enzymes associated with central carbon metabolism, some proteins related to energy conservation and reducing power production showed increased expression under the Cr(VI)-reducing condition. As the best example, $F_{420}H_2$ dehydrogenase (Fpo), an essential protein for the regeneration of $F_{420}H_2$ for energy conservation and electron transportation of ANME [65], saw elevated expression with its subunits including FpoO, FpoN, FpoM, FpoL, FpoC, and FpoB upregulated to 4.7-, 1.7-, 1.5-, 1.3-, 1.3, and 1.2 respectively. Fpo in ANME is closely related to NADH dehydrogenases [65]. The upregulation of Fpo indicated F_{420}

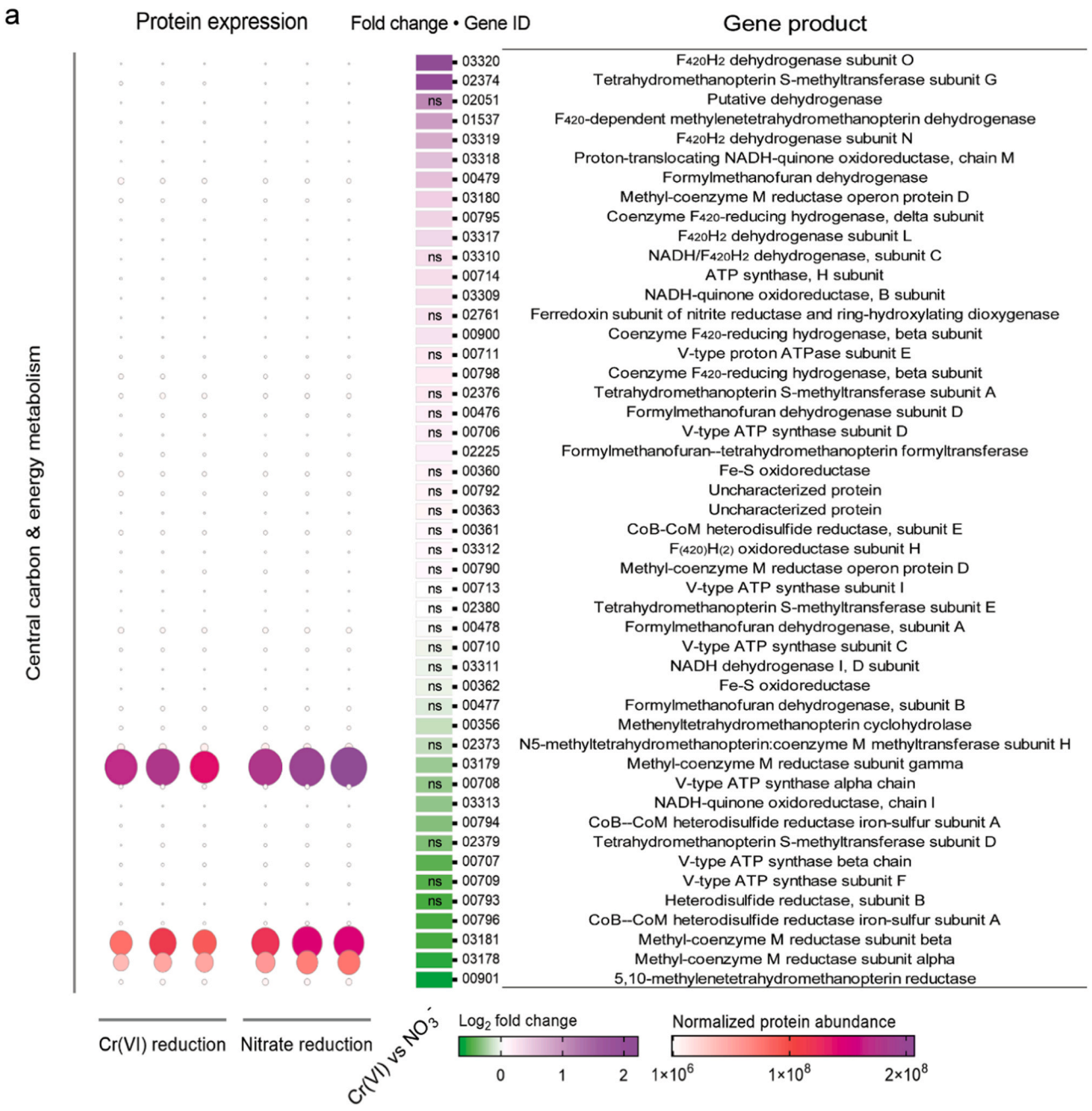

Fig. 6. Quantitative comparison of selected proteins of "*Ca.* Methanoperedens" under Cr(VI)- reducing and nitrate-reducing conditions. **a** Abundance of central carbon and energy metabolism-related proteins. **b** Abundance of terminal electron pathway-related proteins. The normalized protein abundance value represents the total intensity of the protein. Bubble size and colour indicate protein abundance of the corresponding gene product in each biological replicate. Significant difference in fold changes of protein abundance of each condition pair is denoted by asterisks. The full set of quantitative proteomics results is provided in the Supplementary datasheet.

may be the functional cofactor/electron donor in "*Ca.* Methanoperedens" to provide redox equivalents for Cr(VI) reduction, as that of NADH-dependent Cr(VI) reduction by several bacteria [50]. In addition, proton-translocating NADH dehydrogenase (03318), a F_{420} homolog [66], and proteins associated with $F_{420}H_2$ or NADH, including NADH/$F_{420}H_2$ dehydrogenase (03310), NADH-quinone oxidoreductase (03309) also upregulated to 1.5-, 1.3-, and 1.2-fold, respectively. The similar phenomenon of overexpression of proteins associated with reducing power generation for counteracting Cr(VI) exposure has been reported in several bacteria, which was explained as a way to repair cellular damage and Cr(VI) reduction [67].

Regarding proteins involved in terminal electron transfer pathways, "*Ca.* Methanoperedens" cells under Cr(VI)-reducing conditions also showed significantly different features from those under the nitrate-reducing condition. Proteins involved in the nitrate reduction pathway that are highly expressed in nitrate-reducing incubations, including nitrate reductase cytochrome c-type subunit (NapB)/NapC/NirT cytochrome c family (03413), putative respiratory nitrate reductase heme subunit ORF7 (01130), nitrate reductase delta subunit (01129), NapH (01132), and nitrate reductase beta subunit (01128), significantly downregulated to 0.5-, 0.6-, 0.7-, 0.9-, and 0.9-fold, respectively (Fig. 6b). These results indicate that nitrate-reducing proteins embedded

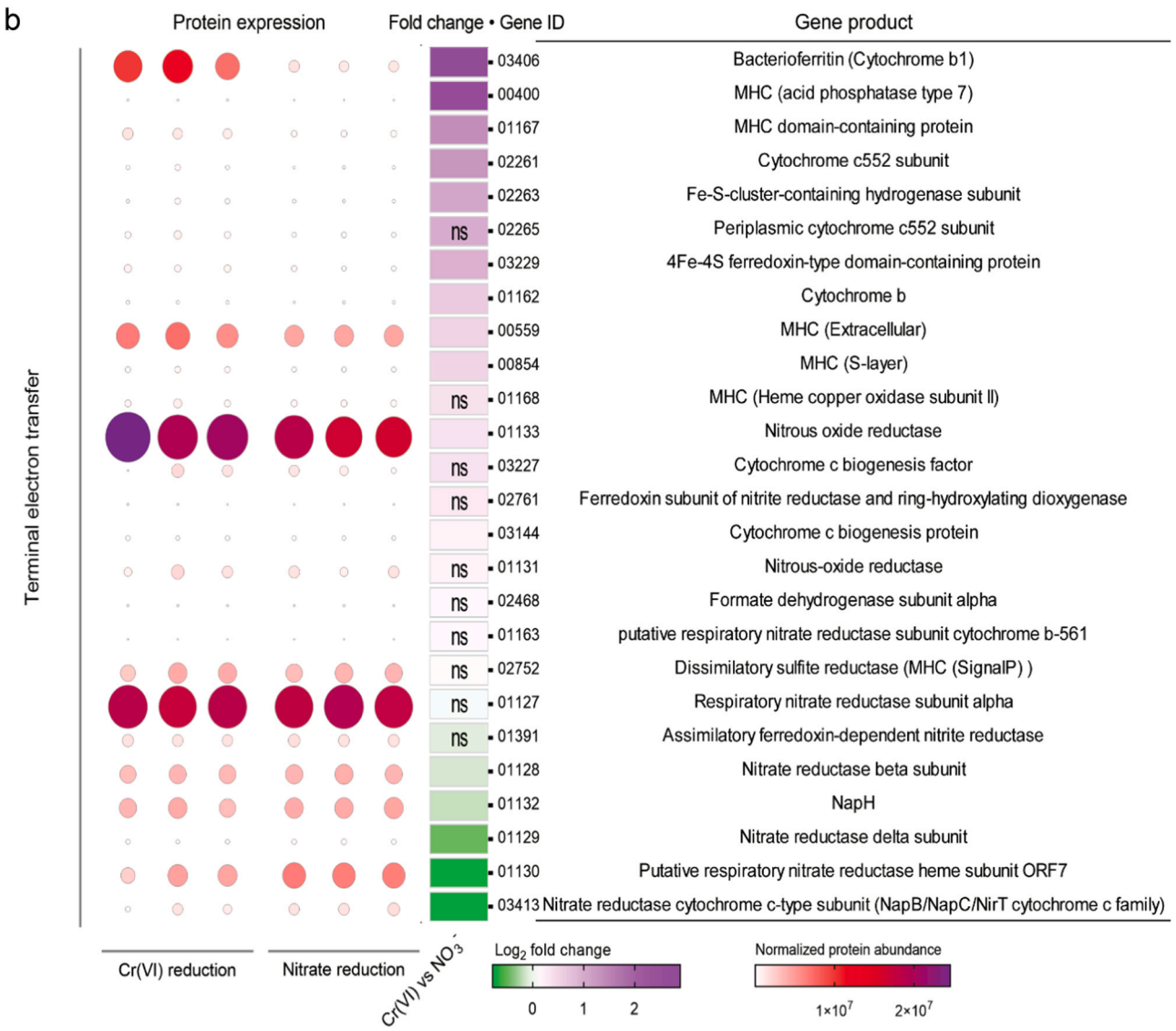

Fig. 6. (*continued*).

in "*Ca*. Methanoperedens" were not responsible for Cr(VI) reduction. By contrast, the regulation of some nitroreductase, including a formate-dependent nitrite reductase (periplasmic cytochrome c552 subunit; 02261) and a nitrous-oxide reductase (01133), were significantly upregulated to 2.4- and 1.3-fold, respectively. A formate-dependent nitrite reductase is previously found to be partly responsible for Cr(VI) reduction by *Shewanella oneidensis* MR-1 [68]. Thus, the formate-dependent nitrite reductase harboured by "*Ca*. Methanoperedens" could contribute to its Cr(VI) reduction, which could be an explanation for the observation of intracellular reductive immobilization of Cr(VI) by "*Ca*. Methanoperedens" (Fig. 3b).

The regulation of the MHC domain-containing proteins seems to reconcile the extracellular reductive immobilization of Cr(VI) by "*Ca*. Methanoperedens". Many MHCs of "*Ca*. Methanoperedens" were among the ten most upregulated proteins in terminal electron transfer pathways during the Cr(VI)-dependent AOM process in comparison to the nitrate condition, including 03406 (7.4-fold), 00400 (6.2-fold), 01167 (2.6-fold), 01162 (1.6-fold), 00559 (1.5-fold), and 00854 (1.4-fold) (Fig. 6b, Supplementary datasheet). Further, MHC quotative analysis revealed that the content of heme proteins under the Cr(VI)-reducing incubation condition (2.42 ± 0.05 μmol/mg·(protein)) was approximately 3.6-fold higher than that measured under nitrate-reducing condition (0.67 ± 0.01 μmol/mg·(protein)) (Fig. S6). More specifically, MHCs (00559) and (00854) are predicted to be extracellularly located [29], which might be the final reductases for extracellular Cr(VI) reduction by "*Ca*. Methanoperedens". Altogether, these MHC expression patterns indicate that "*Ca*. Methanoperedens" can utilize multiple MHCs to facilitate extracellular Cr(VI) reduction.

3.7. Environmental and biotechnological implications

In this study, we provide physiological evidence supporting the ability of "*Ca*. Methanoperedens" to couple AOM to Cr(VI) reduction. Our results further support the metabolic versatility of "*Ca*. Methanoperedens" as previously indicated by the genetic analyses [12]. Given the wide distribution of "*Ca*. Methanoperedens" in natural and engineered ecosystems [69,70], this study suggests AOM-driven Cr(VI) reduction as a previously overlooked but important pathway for chromium immobilization. As the bioavailability and toxicity of Cr(VI) can be significantly reduced as the result of its reduction to Cr(III) [71], this AOM-Cr(VI)-reduction pathway would have important implications for the ecosystem health of methane-abundant chromium-contaminated natural niches such as wetlands, and for food safety by methane-induced chromium immobilization in agriculture soils such as paddy soils.

Further research with more *in-situ* geochemical samples is required to understand the environmental impact of this pathway on local carbon cycles and the detoxication of chromium contaminations in natural systems.

Our results may also support the developments of water treatment technologies aimed at removing chromate from contaminated aquatic environments (e.g., groundwater) or chromate-contained wastewater (e.g., industry wastewater from tanneries, materials, mining, coloring, printing, photographic and medicinal industries [72,73]. In comparison to using organic carbons as electron donors for bioremediation and wastewater treatment, methane can not only provide a more readily available and relatively cost-effective choice [74,75] but also offer the advantage of minimizing secondary pollution [76,77]. EET-capable microorganisms are viewed as promising candidates for reductive Cr(VI) detoxification in wastewater treatment due to their extracellular respiratory pathways to resist Cr(VI) toxicity [30,31,52,56]. Here, we demonstrate for the first time that "*Ca.* Methanoperedens" has a tolerance to Cr(VI) at a comparable level to well-known EET-capable organisms such as *Geobacter* and *Shewanella* (Table S2), indicating the promising applicability of ANME in reductive immobilization of Cr(VI) from wastewater. Despite the similar tolerance to the toxicity, the methane-fuelled Cr(VI) reduction rate by "*Ca.* Methanoperedens" is, however, one to two orders of magnitude lower than that driven by other microorganisms using readily biodegradable organics such as acetate and lactate (Table S2). This distinct contrast could be due to the low methane bioavailability in the water and the limited biomass concentration of "*Ca.* Methanoperedens" enrichment culture. Both limitations could potentially be addressed through the implementation of methane-based membrane biofilm batch reactors (MBfRs). On the one hand, methane in MBfRs is delivered through gas-permeable membranes and methanotrophic biofilm growing on membranes has therefore direct access to methane at supersaturation levels to overcome the low solubility of methane in the solution. On the other hand, membranes in MBfRs offer a large surface area that supports the growth of slow-growing methanotrophs within the biofilm, consequently boosting their activity. On this basis, the implementation of MBfRs has been demonstrated to enhance methane-based denitrification performance by one to two orders of magnitude [78,79]. If this extent of improvement could be similarly adapted for Cr(VI) reduction by "*Ca.* Methanoperedens" as reported in this study, then this methane-fuelled system could be expected to achieve Cr(VI) bioremediation at rates comparable to those driven by other EET-capable microorganisms using readily biodegradable organics (Table S2). Future studies are required to test and optimize Cr(VI) bioremediation by "*Ca.* Methanoperedens" in methane-fuelled MBfRs to evaluate its applicability and robustness for real application.

4. Conclusions

In this study, a "*Ca.* Methanoperedens" enrichment culture was used to investigate the microbiological and biochemical mechanism of methane-fueled Cr(VI) reduction mediated by "*Ca.* Methanoperedens". All findings in this research led to the following take-home messages:

1.11. "*Ca.* Methanoperedens" is capable of performing microbial Cr(VI) reduction independently.
1.12. "*Ca.* Methanoperedens" reduce Cr(VI) dominantly (~94%) using an extracellular respiratory pathway.
1.13. MHCs of "*Ca.* Methanoperedens" provide biochemical foundations for extracellular reductive Cr(VI) immobilization, while the intracellular Cr(VI) reduction may be supported by NAD(P)H/$F_{420}H_2$ associated enzymes and a formate-dependent nitrite reductase.

Environmental implication

This study provides multiple evidence to reveal the coupled anaerobic oxidation of methane (AOM) to Cr(VI) reduction independently by the anaerobic methanotrophic archaea of "*Ca.* Methanoperedens". This finding highlights the important implication for the metabolic versatility of "*Ca.* Methanoperedens". Given the wide distribution of "*Ca.* Methanoperedens" in ecosystems, this pathway has environmental implications for ecosystem health in methane-abundance, chromium-contaminated areas and food safety in agricultural soils. Additionally, it has the implication for developing AOM-based biotechnology using "*Ca.* Methanoperedens" as the biocatalyst for Cr(VI)-contaminated wastewater treatment or groundwater remediation.

CRediT authorship contribution statement

Xueqin Zhang: Writing – review & editing, Writing – original draft, Validation, Supervision, Formal analysis, Conceptualization. **Suicao Wang:** Writing – original draft, Methodology, Investigation, Formal analysis, Data curation. **Jing Zhao:** Writing – review & editing, Visualization, Methodology. **Dihua Tian:** Writing – review & editing, Methodology, Investigation. **Fangrui Cai:** Methodology, Investigation. **Hesamoddin Rabiee:** Visualization, Methodology. **Bernardino Virdis:** Writing – review & editing. **Mengying Xie:** Methodology. **Zhiguo Yuan:** Writing – review & editing, Resources, Funding acquisition. **Jianhua Guo:** Writing – review & editing, Investigation. **Shihu Hu:** Writing – review & editing, Validation, Supervision, Resources, Funding acquisition. **Run Zhang:** Writing – review & editing, Validation, Resources, Methodology.

Declaration of Competing Interest

The authors declare that they have no known competing financial interests or personal relationships that could have appeared to influence the work reported in this paper.

Data Availability

Data will be made available on request.

Acknowledgments

We are grateful to the ACWEB Analytical Services Laboratory (ASL) for the chemical analysis. The authors acknowledge the support from the Centre for Microscopy and Microanalysis (CMM) at UQ for TEM analysis. The authors also acknowledge the Queensland node of Metabolomics Australia at The University of Queensland, an Australian Government initiative through the National Collaborative Research Infrastructure Strategy (NCRIS), under Bioplatforms Australia Pty Ltd., for proteomic analysis. This work is supported by the Australian Research Council (ARC) through an Australian Laureate Fellowship awarded to ZY (FL170100086) and Discovery Project (DP180103595). Z.Y. is Global STEM Scholar funded by the Innovation and Technology Commission of the Government of the Hong Kong Special Administrative Region.

Appendix A. Supporting information

Supplementary data associated with this article can be found in the online version at doi:10.1016/j.jhazmat.2024.136020.

References

[1] Pachauri, R.K., Allen, M.R., Barros, V.R., Broome, J., Cramer, W., Christ, R., et al., 2014. Ipcc. Clim Change 2014: Synth Rep Contrib Work Groups I, II III fifth Assess Rep Intergov Panel Clim Change.

[2] Zhang, X., Yuan, Z., Hu, S., 2021. Anaerobic oxidation of methane mediated by microbial extracellular respiration. Environ Microbiol Rep 13, 790–804.
[3] Knittel, K., Boetius, A., 2009. Anaerobic oxidation of methane: progress with an unknown process. Annu Rev Microbiol 63, 311–334.
[4] Segarra, K., Schubotz, F., Samarkin, V., Yoshinaga, M.Y., Hinrichs, K.-U., Joye, S.B., 2015. High rates of anaerobic methane oxidation in freshwater wetlands reduce potential atmospheric methane emissions. Nat Commun 6, 1–8.
[5] Martinez-Cruz, K., Sepulveda-Jauregui, A., Casper, P., Anthony, K.W., Smemo, K. A., Thalasso, F., 2018. Ubiquitous and significant anaerobic oxidation of methane in freshwater lake sediments. Water Res 144, 332–340.
[6] Shi, L.-D., Wang, Z., Liu, T., Wu, M., Lai, C.-Y., Rittmann, B.E., et al., 2021. Making good use of methane to remove oxidized contaminants from wastewater. Water Res, 117082.
[7] Bhattarai, S., Cassarini, C., Lens, P., 2019. Physiology and distribution of archaeal methanotrophs that couple anaerobic oxidation of methane with sulfate reduction. Microbiol Mol Biol Rev 83 e00074-00018.
[8] Bai, Y., Wang, X., Zhang, F., Zeng, R.J., 2022. Acid orange 7 degradation using methane as the sole carbon source and electron donor. Front Environ Sci Eng 16, 1–9.
[9] Boetius, A., Ravenschlag, K., Schubert, C.J., Rickert, D., Widdel, F., Gieseke, A., et al., 2000. A marine microbial consortium apparently mediating anaerobic oxidation of methane. Nature 407, 623–626.
[10] Haroon, M.F., Hu, S., Shi, Y., Imelfort, M., Keller, J., Hugenholtz, P., et al., 2013. Anaerobic oxidation of methane coupled to nitrate reduction in a novel archaeal lineage. Nature 500, 567–570.
[11] Raghoebarsing, A.A., Pol, A., van de Pas-Schoonen, K.T., Smolders, A.J., Ettwig, K. F., Rijpstra, W.I., et al., 2006. A microbial consortium couples anaerobic methane oxidation to denitrification. Nature 440, 918–921.
[12] Leu, A.O., Cai, C., McIlroy, S.J., Southam, G., Orphan, V.J., Yuan, Z., et al., 2020. Anaerobic methane oxidation coupled to manganese reduction by members of the methanoperedenaceae. ISME J 14, 1030–1041.
[13] Bai, Y.-N., Wang, X.-N., Wu, J., Lu, Y.-Z., Fu, L., Zhang, F., et al., 2019. Humic substances as electron acceptors for anaerobic oxidation of methane driven by ANME-2d. Water Res 164, 114935.
[14] Lai, C.-Y., Wen, L.-L., Shi, L.-D., Zhao, K.-K., Wang, Y.-Q., Yang, X., et al., 2016. Selenate and nitrate bioreductions using methane as the electron donor in a membrane biofilm reactor. Environ Sci Technol 50, 10179–10186.
[15] Lu, Y.Z., Fu, L., Ding, J., Ding, Z.W., Li, N., Zeng, R.J., 2016. Cr(VI) reduction coupled with anaerobic oxidation of methane in a laboratory reactor. Water Res 102, 445–452.
[16] Shi, L.-D., Guo, T., Lv, P.-L., Niu, Z.-F., Zhou, Y.-J., Tang, X.-J., et al., 2020. Coupled anaerobic methane oxidation and reductive arsenic mobilization in wetland soils. Nat Geosci 13, 799–805.
[17] Qu, C., Li, L., Feng, F., Jiang, K., Wu, X., Qin, M., et al., 2023. Enhancement of extracellular Cr (VI) reduction for anammox recovery using hydrazine: performance, pathways, and mechanism. Front Environ Sci Eng 17, 115.
[18] Zhao, M., Wang, X., Wang, S., Gao, M., 2024. Cr-containing wastewater treatment based on Cr self-catalysis: a critical review. Front Environ Sci Eng 18, 1.
[19] Laxmi, V., Kaushik, G., 2020. Toxicity of hexavalent chromium in environment, health threats, and its bioremediation and detoxification from tannery wastewater for environmental safety. Bioremed Ind Waste Environ Saf: Vol I: Ind Waste Manag 223–243.
[20] Qu, J., Chen, J., 2024. Pathways toward a pollution-free planet and challenges. Front Environ Sci Eng 18, 67.
[21] He, X., Wu, C., Qian, Y., Li, Y., Zhang, L., Ding, F., et al., 2019. Highly sensitive and selective light-up fluorescent probe for monitoring gallium and chromium ions in vitro and in vivo. Analyst 144, 3807–3816.
[22] Sharma, P., Singh, S.P., Parakh, S.K., Tong, Y.W., 2022. Health hazards of hexavalent chromium (Cr (VI)) and its microbial reduction. Bioengineered 13, 4923–4938.
[23] Chung, J., Nerenberg, R., Rittmann, B.E., 2006. Bio-reduction of soluble chromate using a hydrogen-based membrane biofilm reactor. Water Res 40, 1634–1642.
[24] Zhou, X., Zhang, Z., Yang, H., 2024. Stabilization/solidification mechanisms of tin tailings and fuming slag-based geopolymers for different heavy metals. Front Environ Sci Eng 18, 1–13.
[25] Zhang, X., Meng, G., Hu, J., Xiao, W., Li, T., Zhang, L., et al., 2023. Electroreduction of hexavalent chromium using a porous titanium flow-through electrode and intelligent prediction based on a back propagation neural network. Front Environ Sci Eng 17, 97.
[26] Dong, Q.Y., Wang, Z., Shi, L.D., Lai, C.Y., Zhao, H.P., 2019. Anaerobic methane oxidation coupled to chromate reduction in a methane-based membrane biofilm batch reactor. Environ Sci Pollut Res Int 26, 26286–26292.
[27] Luo, J.H., Wu, M., Liu, J., Qian, G., Yuan, Z., Guo, J., 2019. Microbial chromate reduction coupled with anaerobic oxidation of methane in a membrane biofilm reactor. Environ Int 130, 104926.
[28] Ettwig, K.F., Van Alen, T., van de Pas-Schoonen, K.T., Jetten, M.S., Strous, M., 2009. Enrichment and molecular detection of denitrifying methanotrophic bacteria of the NC10 phylum. Appl Environ Microbiol 75, 3656–3662.
[29] McIlroy, S.J., Leu, A.O., Zhang, X., Newell, R., Woodcroft, B.J., Yuan, Z., et al., 2023. Anaerobic methanotroph 'Candidatus Methanoperedens nitroreducens' has a pleomorphic life cycle. Nat Microbiol 8, 321–331.
[30] Gong, Y., Werth, C.J., He, Y., Su, Y., Zhang, Y., Zhou, X., 2018. Intracellular versus extracellular accumulation of Hexavalent chromium reduction products by Geobacter sulfurreducens PCA. Environ Pollut 240, 485–492.
[31] Huang, X.-N., Min, D., Liu, D.-F., Cheng, L., Qian, C., Li, W.-W., et al., 2019. Formation mechanism of organo-chromium (III) complexes from bioreduction of chromium (VI) by Aeromonas hydrophila. Environ Int 129, 86–94.
[32] Jiang, T., Bian, W., Kan, J., Sun, Y., Ding, N., Li, W., et al., 2021. Sensitive and rapid detection of Cr3+ in live cells by a red turn-on fluorescent probe. Spectrochim Acta Part A: Mol Biomol Spectrosc 245, 118903.
[33] Arshad, A., Speth, D.R., de Graaf, R.M., Op den Camp, H.J., Jetten, M.S., Welte, C. U., 2015. A metagenomics-based metabolic model of nitrate-dependent anaerobic oxidation of methane by Methanoperedens-like archaea. Front Microbiol 6, 1423.
[34] Zhang, X., Joyce, G.H., Leu, A.O., Zhao, J., Rabiee, H., Virdis, B., et al., 2023. Multi-heme cytochrome-mediated extracellular electron transfer by the anaerobic methanotroph 'Candidatus Methanoperedens nitroreducens'. Nat Commun 14, 6118.
[35] Frank, J., Zhang, X., Marcellin, E., Yuan, Z., Hu, S., 2023. Salinity effect on an anaerobic methane-and ammonium-oxidising consortium: shifts in activity, morphology, osmoregulation and syntrophic relationship. Water Res, 120090.
[36] M.-T. Hopp , B.F. Schmalohr , T. Kuhl, M.S. Detzel, A. Wißbrock, D. Imhof, Heme determination and quantification methods and their suitability for practical applications and everyday use, in, ACS Publications, 2020.
[37] Fr/Olund, B., Griebe, T., Nielsen, P., 1995. Enzymatic activity in the activated-sludge floc matrix. Appl Microbiol Biotechnol 43, 755–761.
[38] Engelbrektson, A., Kunin, V., Wrighton, K.C., Zvenigorodsky, N., Chen, F., Ochman, H., et al., 2010. Experimental factors affecting PCR-based estimates of microbial species richness and evenness. ISME J 4, 642–647.
[39] Zhang, X., Xia, J., Pu, J., Cai, C., Tyson, G.W., Yuan, Z., et al., 2019. Biochar-mediated anaerobic oxidation of methane. Environ Sci Technol 53, 6660–6668.
[40] Frank, J., Zhang, X., Marcellin, E., Yuan, Z., Hu, S., 2023. Salinity effect on an anaerobic methane-and ammonium-oxidising consortium: Shifts in activity, morphology, osmoregulation and syntrophic relationship. Water Res 242, 120090.
[41] Gong, Y.-F., Song, J., Ren, H.-T., Han, X., 2015. Comparison of Cr (VI) removal by activated sludge and dissolved organic matter (DOM): importance of UV light. Environ Sci Pollut Res 22, 18487–18494.
[42] Scheller, S., Yu, H., Chadwick, G.L., McGlynn, S.E., Orphan, V.J., 2016. Artificial electron acceptors decouple archaeal methane oxidation from sulfate reduction. Science 351, 703–707.
[43] Cooke, V.M., Hughes, M.N., Poole, R.K., 1995. Reduction of chromate by bacteria isolated from the cooling water of an electricity generating station. J Ind Microbiol 14, 323–328.
[44] Elangovan, R., Abhipsa, S., Rohit, B., Ligy, P., Chandraraj, K., 2006. Reduction of Cr (VI) by a Bacillus sp. Biotechnol Lett 28, 247–252.
[45] Okeke, B.C., Laymon, J., Crenshaw, S., Oji, C., 2008. Environmental and kinetic parameters for Cr (VI) bioreduction by a bacterial monoculture purified from Cr (VI)-resistant consortium. Biol Trace Elem Res 123, 229–241.
[46] Long, D., Tang, X., Cai, K., Chen, G., Chen, L., Duan, D., et al., 2013. Cr (VI) reduction by a potent novel alkaliphilic halotolerant strain Pseudochrobactrum saccharolyticum LY10. J Hazard Mater 256, 24–32.
[47] Wu, M., Li, Y., Li, J., Wang, Y., Xu, H., Zhao, Y., 2019. Bioreduction of hexavalent chromium using a novel strain CRB-7 immobilized on multiple materials. J Hazard Mater 368, 412–420.
[48] Liu, T., Li, X., Li, F., Han, R., Wu, Y., Yuan, X., et al., 2016. In situ spectral kinetics of Cr (VI) reduction by c-type cytochromes in a suspension of living Shewanella putrefaciens 200. Sci Rep 6, 29592.
[49] Meng, Y., Ma, X., Luan, F., Zhao, Z., Li, Y., Xiao, X., et al., 2022. Sustainable enhancement of Cr(VI) bioreduction by the isolated Cr(VI)-resistant bacteria. Sci Total Environ 812, 152433.
[50] Pradhan, S.K., Singh, N.R., Rath, B.P., Thatoi, H., 2016. Bacterial chromate reduction: a review of important genomic, proteomic, and bioinformatic analysis. Crit Rev Environ Sci Technol 46, 1659–1703.
[51] Thatoi, H., Das, S., Mishra, J., Rath, B.P., Das, N., 2014. Bacterial chromate reductase, a potential enzyme for bioremediation of hexavalent chromium: a review. J Environ Manag 146, 383–399.
[52] Ngwenya, N., Chirwa, E., 2011. Biological removal of cationic fission products from nuclear wastewater. Water Sci Technol 63, 124–128.
[53] Liu, T., Li, X., Li, F., Han, R., Wu, Y., Yuan, X., et al., 2016. In situ spectral kinetics of Cr(VI) reduction by c-type cytochromes in a suspension of living Shewanella putrefaciens 200. Sci Rep 6, 29592.
[54] Yu, H., He, Z., He, Z., Yan, Q., Shu, L., 2022. Soil amoebae affect iron and chromium reduction through preferential predation between two metal-reducing bacteria. Environ Sci Technol 56, 9052–9062.
[55] Goulhen, F., Gloter, A., Guyot, F., Bruschi, M., 2006. Cr (VI) detoxification by Desulfovibrio vulgaris strain Hildenborough: microbe–metal interactions studies. Appl Microbiol Biotechnol 71, 892–897.
[56] Belchik, S.M., Kennedy, D.W., Dohnalkova, A.C., Wang, Y., Sevinc, P.C., Wu, H., et al., 2011. Extracellular reduction of hexavalent chromium by cytochromes MtrC and OmcA of Shewanella oneidensis MR-1. Appl Environ Microbiol 77, 4035–4041.
[57] Ouboter, H.T., Berben, T., Berger, S., Jetten, M.S., Sleutels, T., Ter Heijne, A., et al., 2022. Methane-dependent extracellular electron transfer at the bioanode by the anaerobic archaeal methanotroph "Candidatus Methanoperedens". Front Microbiol 13, 820989.
[58] Zhang, X., Rabiee, H., Frank, J., Cai, C., Stark, T., Virdis, B., et al., 2020. Enhancing methane oxidation in a bioelectrochemical membrane reactor using a soluble electron mediator. Biotechnol Biofuels 13, 173.
[59] Zhang, X., Rabiee, H., Ni, G., Frank, J., Zhao, J., Cai, C., et al., 2022. Bio-reduced graphene oxide on hollow fibers as gas-diffusible anodes for enhancing bioelectrochemical methane oxidation. Chem Eng J 440.

[60] Zhang, X., Zhao, J., Erler, D.V., Rabiee, H., Kong, Z., Wang, S., et al., 2024. Characterization of the redox-active extracellular polymeric substances in an anaerobic methanotrophic consortium. J Environ Manag 365, 121523.
[61] Zhang, X., Xie, M., Cai, C., Rabiee, H., Wang, Z., Virdis, B., et al., 2023. Pyrogenic carbon promotes anaerobic oxidation of methane coupled with iron reduction via the redox-cycling mechanism. Environ Sci Technol 57, 19793–19804.
[62] Ouboter, H.T., Mesman, R., Sleutels, T., Postma, J., Wissink, M., Jetten, M.S., et al., 2024. Mechanisms of extracellular electron transfer in anaerobic methanotrophic archaea. Nat Commun 15, 1477.
[63] Shima, S., Krueger, M., Weinert, T., Demmer, U., Kahnt, J., Thauer, R.K., et al., 2012. Structure of a methyl-coenzyme M reductase from Black Sea mats that oxidize methane anaerobically. Nature 481, 98–101.
[64] M.F. Haroon , S. Hu , Y. Shi , M. Imelfort , J. Keller , P. Hugenholtz et al. , Erratum: Anaerobic oxidation of methane coupled to nitrate reduction in a novel archaeal lineage (Nature (2013) 500 (567–570) doi:10.1038/nature12375), Nature, 501 (2013) 578.
[65] Wang, F.-P., Zhang, Y., Chen, Y., He, Y., Qi, J., Hinrichs, K.-U., et al., 2014. Methanotrophic archaea possessing diverging methane-oxidizing and electron-transporting pathways. ISME J 8, 1069–1078.
[66] Deppenmeier, U., Lienard, T., Gottschalk, G., 1999. Novel reactions involved in energy conservation by methanogenic archaea. FEBS Lett 457, 291–297.
[67] Viti, C., Marchi, E., Decorosi, F., Giovannetti, L., 2014. Molecular mechanisms of Cr (VI) resistance in bacteria and fungi. FEMS Microbiol Rev 38, 633–659.
[68] Viamajala, S., Peyton, B.M., Apel, W.A., Petersen, J.N., 2002. Chromate/nitrite interactions in Shewanella oneidensis MR-1: Evidence for multiple hexavalent chromium [Cr (VI)] reduction mechanisms dependent on physiological growth conditions. Biotechnol Bioeng 78, 770–778.
[69] Ino, K., Hernsdorf, A.W., Konno, U., Kouduka, M., Yanagawa, K., Kato, S., et al., 2018. Ecological and genomic profiling of anaerobic methane-oxidizing archaea in a deep granitic environment. ISME J 12, 31–47.
[70] Shen, L.-d, Wu, H.-s, Liu, X., Li, J., 2017. Cooccurrence and potential role of nitrite- and nitrate-dependent methanotrophs in freshwater marsh sediments. Water Res 123, 162–172.
[71] Narayani, M., Shetty, K.V., 2013. Chromium-resistant bacteria and their environmental condition for hexavalent chromium removal: a review. Crit Rev Environ Sci Technol 43, 955–1009.
[72] GracePavithra, K., Jaikumar, V., Kumar, P.S., SundarRajan, P., 2019. A review on cleaner strategies for chromium industrial wastewater: present research and future perspective. J Clean Prod 228, 580–593.
[73] Zhang, X., Zhang, Y., Zhu, D., Lin, Z., Sun, N., Su, C., et al., 2023. Chromium phytoextraction and physiological responses of the hyperaccumulator Leersia hexandra Swartz to plant growth-promoting rhizobacterium inoculation. Front Environ Sci Eng 17, 9.
[74] Modin, O., Fukushi, K., Yamamoto, K., 2007. Denitrification with methane as external carbon source. Water Res 41, 2726–2738.
[75] Meulepas, R.J., Stams, A.J., Lens, P.N., 2010. Biotechnological aspects of sulfate reduction with methane as electron donor. Rev Environ Sci Bio/Technol 9, 59–78.
[76] Chen, H., Liu, S., Liu, T., Yuan, Z., Guo, J., 2020. Efficient nitrate removal from synthetic groundwater via in situ utilization of short-chain fatty acids from methane bioconversion. Chem Eng J 393, 124594.
[77] Luo, J.-H., Wu, M., Yuan, Z., Guo, J., 2017. Biological bromate reduction driven by methane in a membrane biofilm reactor. Environ Sci Technol Lett 4, 562–566.
[78] Cai, C., Hu, S., Guo, J., Shi, Y., Xie, G.-J., Yuan, Z., 2015. Nitrate reduction by denitrifying anaerobic methane oxidizing microorganisms can reach a practically useful rate. Water Res 87, 211–217.
[79] Xie, G.-J., Cai, C., Hu, S., Yuan, Z., 2017. Complete nitrogen removal from synthetic anaerobic sludge digestion liquor through integrating anammox and denitrifying anaerobic methane oxidation in a membrane biofilm reactor. Environ Sci Technol 51, 819–827.